Molecular Crystals and Liquid Crystals Science and Technology. Section A. Molecular Crystals and Liquid Crystals

Publication details, including instructions for authors and subscription information:
http://www.tandfonline.com/loi/gmcl19

C.W. Optical Frederiks Transition: Thermal Effect and Surface Director Reorientation; T.I.R. Investigations

M. Warenghem [a], M. Ismaili [a], F. Simont [a b], F. Bloist [a b] & L. Vicari [a b]

[a] Laboratoire de Dynamique et Structure des Matériaux Moléculaires, U.R.A. C.N.R.S. 801; U.S.T.L.; F.59655, VILLENEUVE D'ASCQ, Cedex

[b] Dipartimento di Scienze Fisiche;, Università di Napoli;, Piazzale Tecchio 80, 80125, NAPOLI, ITALY

Version of record first published: 24 Sep 2006.

To cite this article: M. Warenghem , M. Ismaili , F. Simont , F. Bloist & L. Vicari (1994): C.W. Optical Frederiks Transition: Thermal Effect and Surface Director Reorientation; T.I.R. Investigations, Molecular Crystals and Liquid Crystals Science and Technology. Section A. Molecular Crystals and Liquid Crystals, 251:1, 43-59

To link to this article: http://dx.doi.org/10.1080/10587259408027191

Mol. Cryst. Liq. Cryst. 1994, Vol. 251, pp. 43–59
Reprints available directly from the publisher
Photocopying permitted by license only

Printed in the United States of America

C.W. OPTICAL FREDERIKS TRANSITION: THERMAL EFFECT AND SURFACE DIRECTOR REORIENTATION; T.I.R. INVESTIGATIONS.

M. WARENGHEM, M. ISMAILI, F. SIMONI*, F. BLOISI*, L. VICARI*

Laboratoire de Dynamique et Structure des Matériaux Moléculaires
U.R.A. C.N.R.S. 801; U.S.T.L.; F.59655, VILLENEUVE D'ASCQ Cedex
*Dipartimento di Scienze Fisiche; Università di Napoli; Piazzale Tecchio 80
80125 NAPOLI, ITALY

Abstract Quantitative results on optically induced director reorientation in an homeotropically aligned nematic film illuminated with the green line of an argon laser pump beam is presented. Total internal reflection has been used to measure both ordinary and extraordinary refractive indices and therefrom have been deduced first, the temperature profiles of the nematic within the illuminated region and second the surface tilt angle of the director, both for different pump powers. The temperature profiles have been found to be quite well fitted using gaussian shapes. The surface tilt angle in the center of the pump beam linearly depends on the pump power with a quasi threshold behavior depending on the anchoring energies.

INTRODUCTION

As it is well known now, an electromagnetic wave travelling through a nematic film experiences a phase distorsion that is intensity dependent : the nematic film is a photorefractive material and it can be focusing, diffracting or defocusing. The mechanism of photorefractivity can be either an induced thermal gradient, a collective dielectric reorientation (the so-called Optical Frederiks Transition; O.F.T.) or both. Although many papers dealing with this effect[1] have already been published, most of them use assumptions on how large is the director reorientation or how the thermal dependence affects experimental measurements of pure director reorientation. In

addition, strong anchoring conditions for the nematic film are usually assumed. In the case of O.F.T. generated by short lasers pulses, the assumption of small perturbations is probably reasonnable, but as the pulse is lastening longer or a C.W. laser is used, it might be no longer valid. In this paper, we report experimental measurements of the temperature change within the pump beam due to absorption and the light induced surface director reorientation of weakly anchored nematic film in a geometry with a volume threshold and under continuous pump illumination.

All the results are derived from Total Internal Reflection experiments: therefore, in the first part, the setup that allows to record reflectivity curves is described. It is explained what can be derived from these curves: mainly refractive indices and equal thickness interference patterns. We show how these informations can be turned into temperature and tilt angle measurement. In the second part, the results obtained for 5CB films are presented.

I. EXPERIMENTAL: setup, method and miscellaneous.

Setup.

The setup is shown in figure 1: it is a usual Total Internal Reflection (T.I.R.) one. The nematic film is deposited onto the upper face of a dense prism. A low power He-Ne laser beam (probe beam) is reflected at the nematic-prism interface. The reflected intensity is recorded by means of a photosensor. The angle of incidence can be varied by rotating the mirrors mounted on gimbals; the prism is therefore lifted up or down to illuminate the sample always at the same place. A polariser is inserted in the field to excite either the TE or TM modes. In the chosen geometry, the nematic is supposed to be distorded by the pump beam (as it will be shown in a next figure) in the plane of incidence of the probe beam, therefore, the TE mode corresponds to the ordinary wave in the nematic, whereas the TM mode excites the extraordinary wave. Typically an experiment consists of recording the intensity reflected at the sample interface against the angle of incidence, for both polarisations of the probe beam.

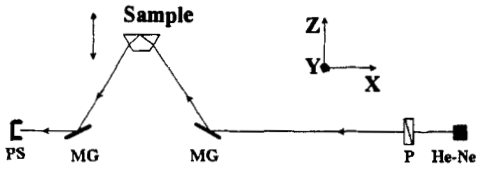

PS: photosensor; P: polariser; MG: mirror gimbal

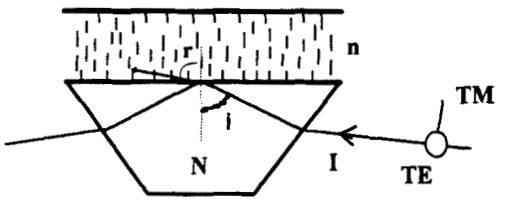

FIGURE 1 T.I.R. setup; up: side view; down: sample closer view.

A typical curve is shown in figure 2 where one can see the T.I.R. regime on the right side and the transmission regime on the left.

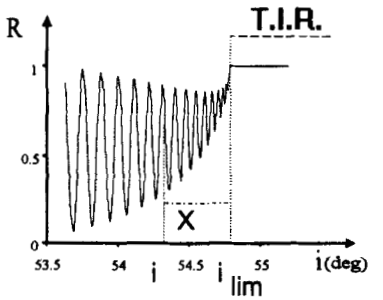

FIGURE 2 General trend of reflectivity curve.

Method.

The Snell-Descartes law applied to the incidence angle which limits both regimes gives the refractive index of the material deposited onto the prism: it is an Abbe or Pulfrich refractometer. In case of a birefringent material and for our geometry, the TE mode, that is to say the ordinary wave, gives to us the ordinary index. This index only

depends on temperature and by comparing the obtained value with a set of values obtained elsewhere[2], one can deduce the surface temperature.

For the TM mode, the extraordinary ray, we have to account for energy and not phase propagation direction and the Snell law properly applied is given by the expression below:

$$N^2 \sin^2(i_l) = n_o^2(T).\sin^2(\theta_s) + n_e^2(T).\sin^2(\theta_s) \qquad 1$$

where θ_S is the surface tilt angle of the optical axis, n_e and n_O are the temperature dependent principal refractive indices of the nematic, i_l is the limit angle between the T.I.R. and transmission regimes and N is the refractive index of the prism. Therefrom, the limit angle measurement for this polarisation gives the surface tilt angle[3]. In the relation 1 the temperatures were obtained as described above .

Thus the limit angle readily gives informations on the surface, but the sample must be checked in the bulk to be sure that the conditions of an initially homeotropically aligned nematic film and an in-plane of incidence distorsion under pump beam influence are fulfilled. It is possible to obtain further informations on what happens in the bulk by probing the volume, that is to say, by processing the data obtained in the transmission regime. The leftmost part of the reflectivity curve shown in figure 2 is an equal thickness fringe pattern and here, we are interested in two possible situations shown in figure 3. The first situation is that of a homogeneous nematic film where the pattern corresponds to interference between the beam reflected at the prism-nematic interface and that reflected at the sample upper interface (Fig. 3a). The second case is that of a distorded film: there is an index gradient and the transmitted beam is totally reflected within the sample (Fig. 3b).

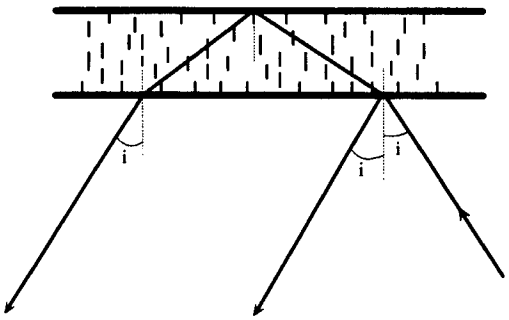

FIGURE 3a Beams interfering in case of a homogeneous nematic film.

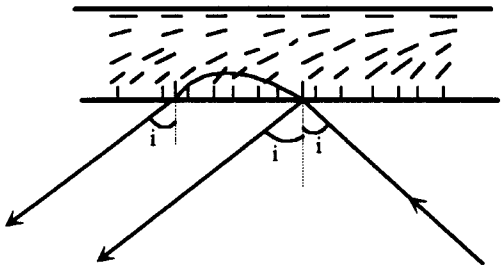

FIGURE 3b Beams interfering in case of a heterogeneous nematic film.

In both cases, the phase difference between the two beams or the order of interference is expressed as below:

$$\frac{\Phi}{2.\pi} = \frac{1}{\lambda}\int_0^e n(\theta, r).\cos(r).dz + \frac{1}{\lambda}\int_e^0 n(\theta', r').\cos(r').dz \qquad 2$$

where the first integral corresponds to the part of the transmitted beam going up and the second to that going down, θ and r are respectively the local optical axis tilt angle and local refraction angle with respect to the normal to the interface; e is the limit of the integral that can be either the total thickness or a part of it.

This integral has been extensively calculated for different geometries[4] and the results are just summed up using the reduced angular abscissa X introduced by Eidner[5] and defined as below:

$$X = \sqrt{N^2.\sin^2(i_{lim}) - N^2.\sin^2(i)} \qquad 3$$

where N is the refractive index of the prism, i is the angle of incidence and i_{lim} is the limit between T.I.R. and transmission regime.

For the ordinary wave (TE mode), the order of interference is found to be linearly dependent on X, with a slope equal to $2.(e/\lambda)$.

For the extraordinary wave (TM mode) and for a homogeneous film, the order of interference is also linearly dependent on X with a slope equal to $2.(e/\lambda).(n_o/n_e)$ for an homeotropically aligned nematic film and $2.(e/\lambda).(n_e/n_o)$ for a planar sample. But in case of a distorded nematic film, the dependence goes with X^2, at least close to the interface.

Therefore, let us consider now an experimental curve. From a selected minimum of the intensity to the next one, the order of interference changes by unity; thus we plot integers on the y-axis and the associated experimental value of X on the x-axis. The obtained curve is either a straight line or a curved one.

We first process the ordinary reflectivity curve: we should find a straight line; if it is not the case, that means that the director is tilted out of the plane of incidence and such a sample is disregarded. If it is a line, the slope gives to us the actual thickness of the film.

Second we process the extraordinary reflectivity curve: if one obtains a line that means the film is unperturbed and if it is not there exists a gradient. At that point, as the film is found to be distorded, a more sophisticated data processing can be used[6,7]. It allows to obtain the director distribution within the sample from our experimental curves without theoretical model. It should be noticed that the processing converges only if the film is distorded and checking the sample as presented above is necessary. This bulk distorsion determination is presented in an another paper[8]. As the film is found distorded, the relation 1 is used to obtain the surface tilt angle.

Miscellaneous.

The actual setup that has been used for this photorefractivity characterisation is shown in figure 4: it looks the same as in the figure 1, but few components have been added.

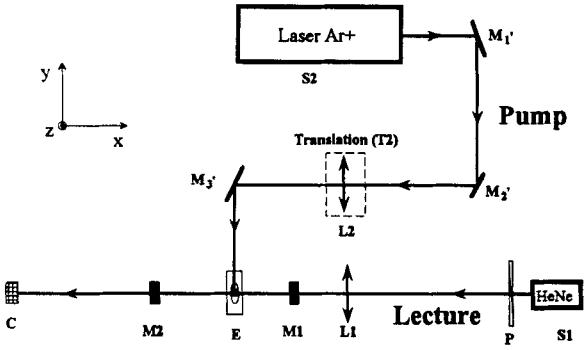

Top view

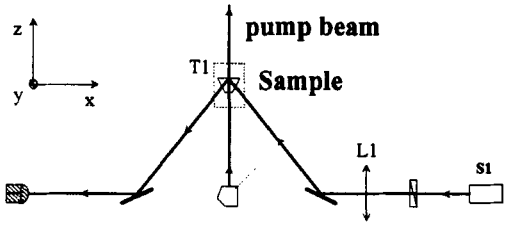

Side view

FIGURE 4. Actual set-up used for nematic film photorefractivity characterisation.

First the pump beam has been carried on the sample under normal incidence and the polarisation has been set in the plane of incidence of the probe beam. Second, to obtain a pump beam powerful enough to act on the molecules, a lens (f = 80 cm) has been inserted in the optical path. This lens has been mounted on a translation stage that is

moving exactly the same way as the sample itself to insure the intensity illuminating the film to be constant. The pump beam radius has been estimated to be 130 micrometers. We have also inserted a lens (f = 60 cm) in the probe beam path to probe an area of the sample as small as possible. This lens has been mounted at a distance of 10 m far from the laser itself and the lecture spot radius has been estimated to be 45 micrometers. The effective power illuminating the sample has been measured and found to be proportionnal to the output laser power.

The homeotropic alignment of the nematic has been achieved using the HTAB technique. With such a geometry, the Optical Frederiks Transition occurs above a threshold. The critical pump power is known to depend on the ratio of the pump radius over the sample thickness. In our experiment, this ratio was around 1.5 and the threshold was 250mW.

2. RESULTS.

We have recorded ordinary and extraordinary curves for different pump powers at different positions of the probe beam with respect to the pump beam.

We first checked the sample in the absence of pump illumination. The ordinary reflectivity curve and the corresponding order of interference curve versus X are shown in figure 5. It is a very nice straight line; also a line has been found for the extraordinary curve, therefore this sample is initially homeotropic with a thickness of 76.8μm. Now as the sample is found initially homeotropic, it can be illuminated and reflectivity curves are recorded for different pump powers at different positions of the lecture spot with respect to the pump beam.

First, the TE mode (ordinary wave) set of curves has been processed to deduce the temperature change profiles within the pump beam.

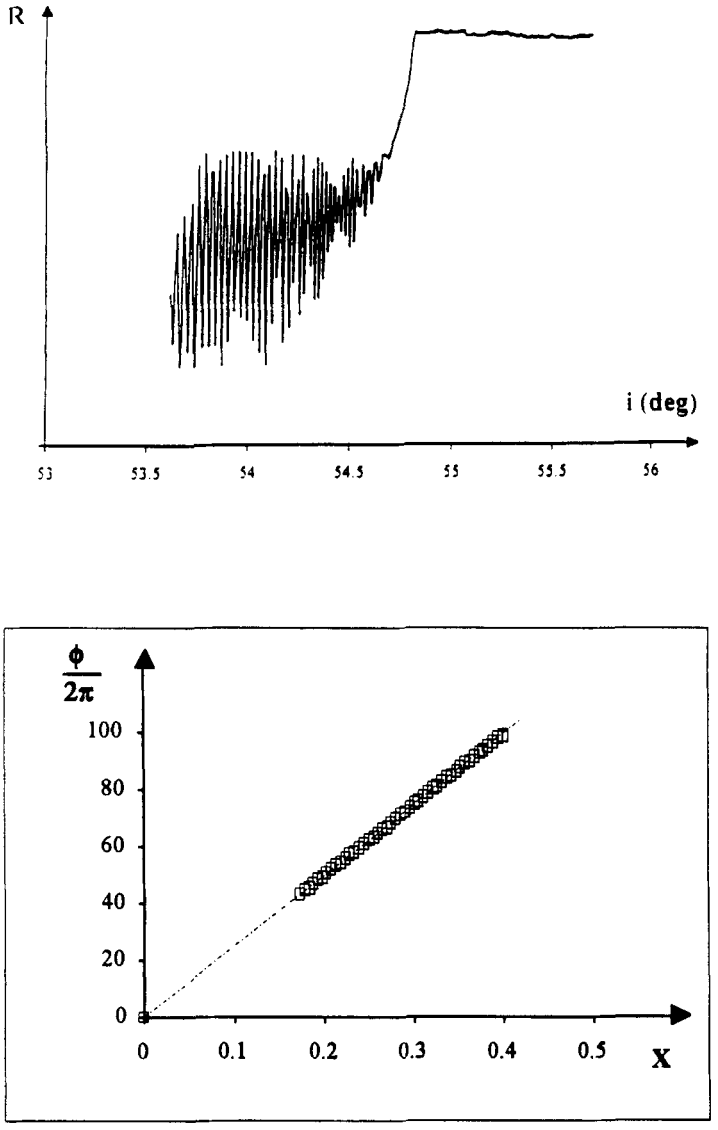

FIGURE 5 Checking the sample in absence of illumination. Top: reflectivity curve; bottom: order of interference.

As an example, in figure 6 the curves obtained for a fixed power and different probe beam positions have been reported. It can be seen that the limit angle shifts back and

forth, indicating changes of the ordinary index and therefore temperature changes across the pump beam section.

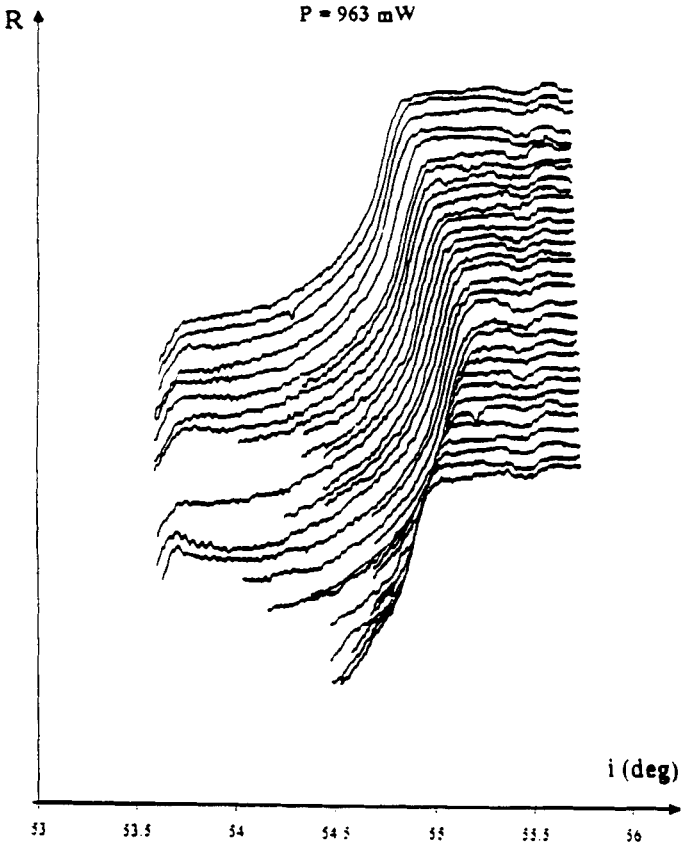

FIGURE 6 Set of reflectivity curves (TE mode) for one pump power and different positions of the probe beam.

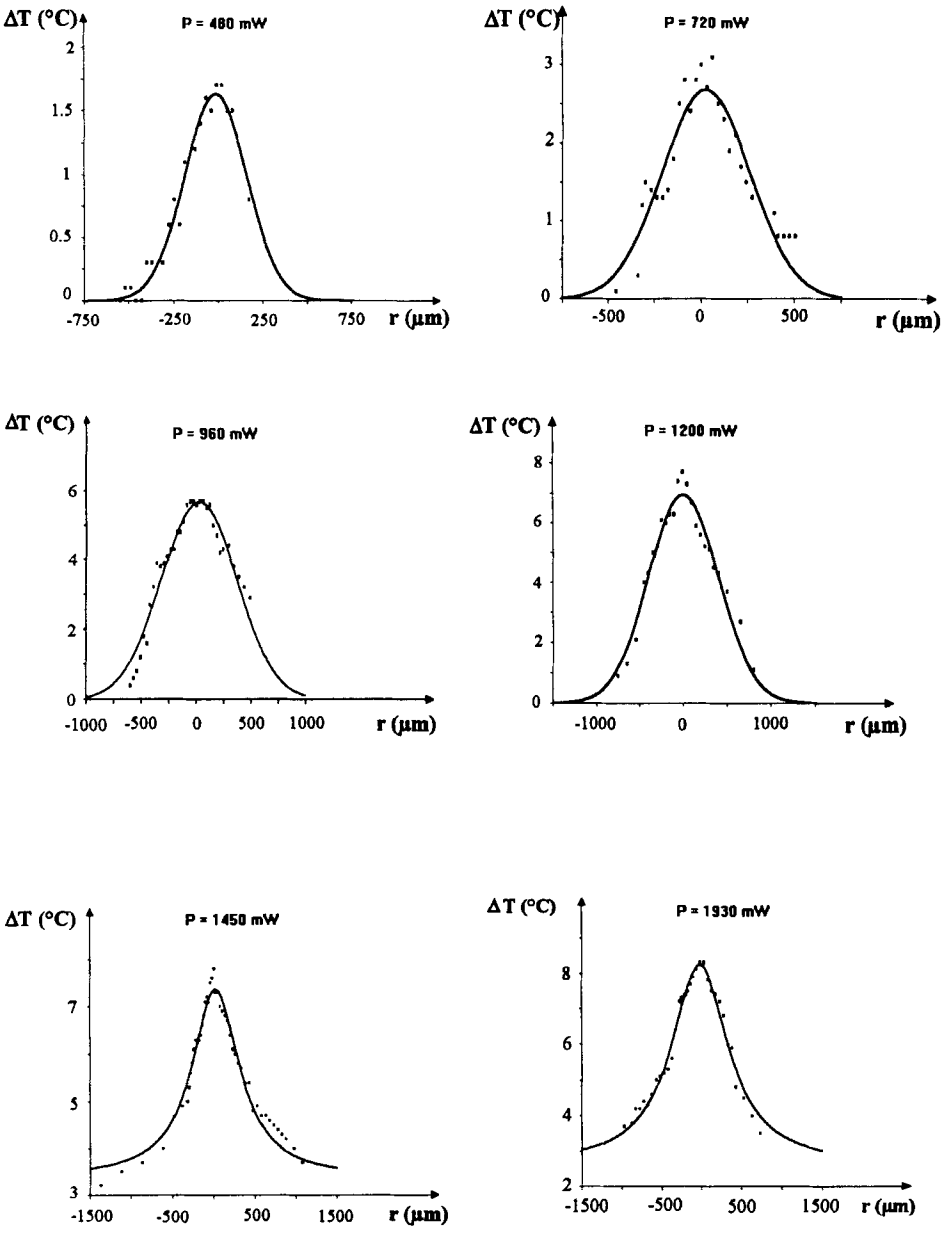

FIGURE 7 Temperature change profiles for different pump powers.

The temperature profiles obtained from these curves for different pump powers are shown in figure 7. For low powers (P = 480, 720, 960, 1200 mW), these profiles are

quite well fitted using gaussian shapes whereas, for higher powers, gaussian shapes still fit the data if translated along the y-axis by two-three degres. The half widths of the fits against the pump power are shown in figure 8. For low powers, the dependence is quasi linear and for higher power, the dependence is still linear but with a lower slope.

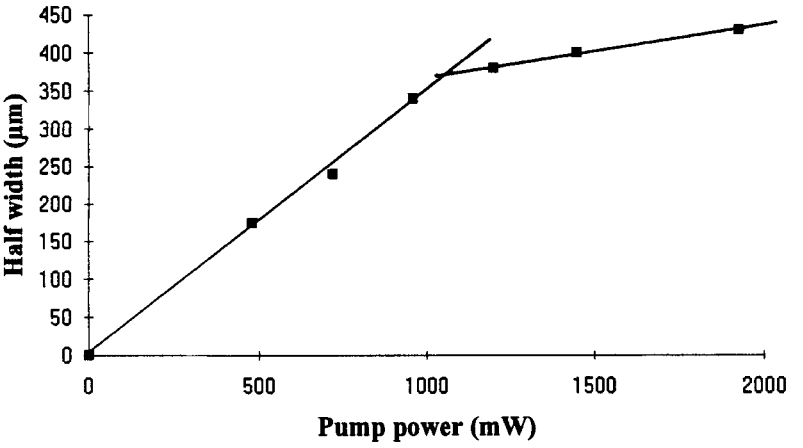

FIGURE 8 Half widths of gaussian shapes that fit the temperature profiles.

The maximum temperature change, that is to say the change at the middle of the pump beamversus the pump power, has also been plotted in figure 9. The origin corresponds to room temperature and for this experiment the isotropic phase transition occurs at 9.8 degrees of temperature rise. Therefore all data refer to the nematic phase. As it can be seen, some saturation occurs above a power which is the same as that separates the two regimes observed on the half width curve (Fig. 8). One can explain that roughly by considering that we approach the phase transition and increasing the temperature by one degree require more energy than far from the transition. However, that does not explain why the half witdh also bend this way.

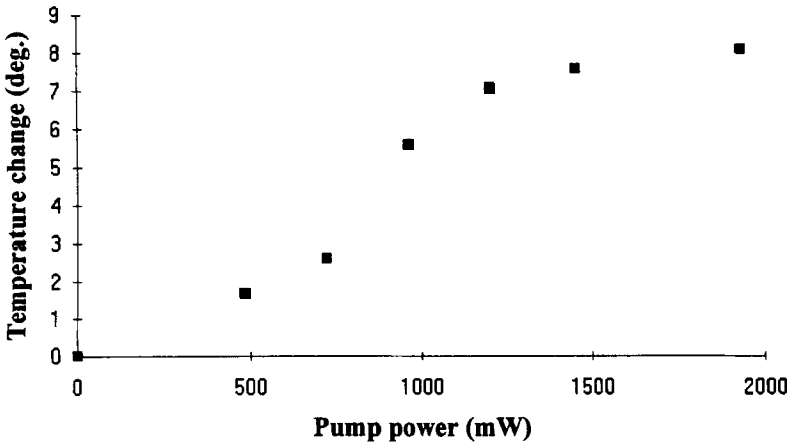

FIGURE 9 Temperature change at the center of the pump beam.

A better explanation can be given by considering the heat transfer problem. At low powers, the sample is homogeneous and the heat transfer is ruled by the perpendicular conductivity coefficient. As the power is increasing, the director rotates and for high power, the film is strongly distorded with a large surface tilt angle and a large bulk tilt angle profile, therefore it is now the parallel heat conductivity coefficient that intervenes. This coefficient is larger than the perpendicular one. For instance Villanove[9] has measured these coefficients for MBBA and found a ratio $D_{\Pi} / D_{\perp}$ equals to 1.65. Thus the heat transfer in a direction parallel to the interface is now much more easy and that explains why we have a baseline in the profile: the whole nematic film has higher temperature. The steady state is solution of the equation 4 that must be coupled with that of the director tilt angle equation, obtained from minimizing the free energy.

$$\mathrm{div}(\bar{\bar{D}}.\vec{\mathrm{grad}}(T)) = -\alpha.I(r) \qquad 4$$

where $\bar{\bar{D}}$ is the thermal conductivity tensor, T the scalar temperature field, α the absorption coefficient and I(r) the light intensity distribution. The dichroism should certainly also act in the process[10] and that modifies the second term in the equation 4.

Other fits better than these presented here have been found for the temperature profiles that should help to solve at least partly the equation 4: this problem is currently under way and will be the topic of a further paper.

The temperature change induced by light absorption being now known, the TM mode set of curves can be processed, in other words, the surface director tilt angle can be deduced from these curves.

Figure 10 shows a set of curves recorded at the center of the pump beam for different pump powers. The limit angle shifts indicating an extraordinary index change.

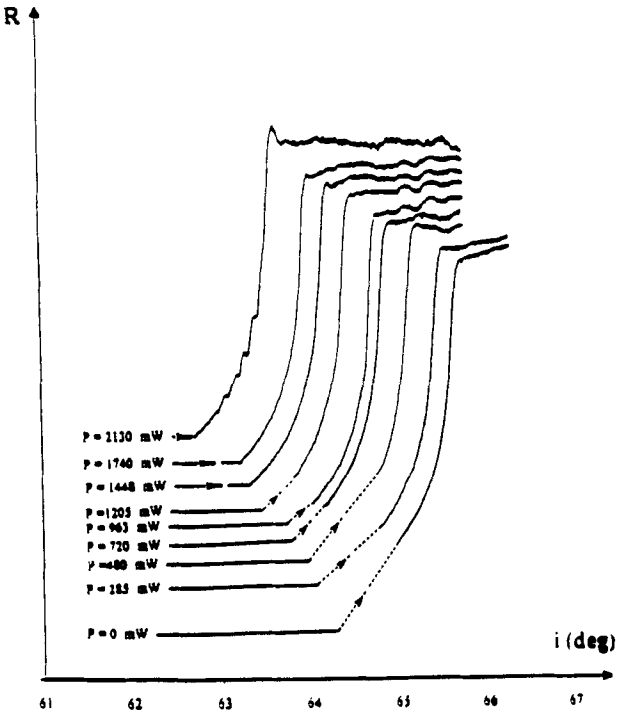

FIGURE 10 TM mode: Reflectivity curves recorded in the center of the pump beam for different pump powers.

The thermal contribution to this change is known from the ordinary set of curves and the surface tilt angle has been derived from these curves, using the relation 1. The

obtained values have been plotted against the pump power for two different samples in figure 11.

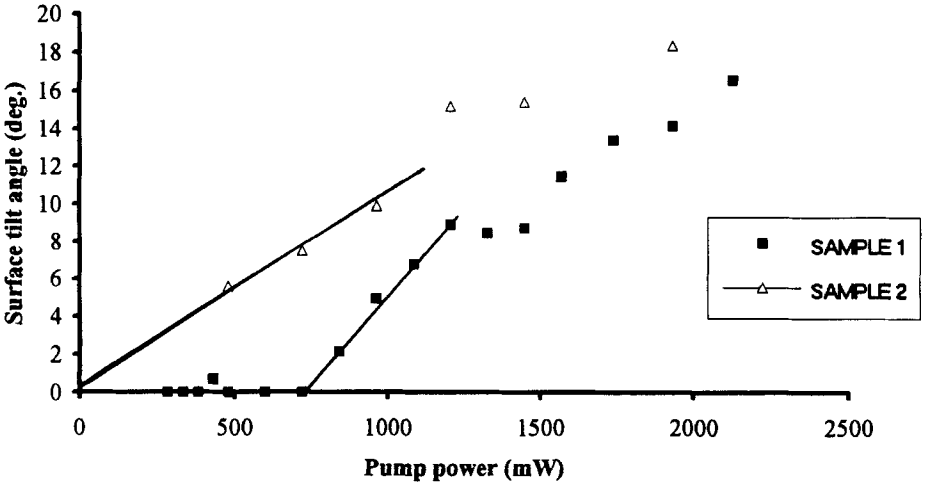

FIGURE 11 Surface tilt angle in the center of the pump beam.

In connection with the obtained results, the followings should be remarked. First, for both samples and low powers (<1000mW), the surface tilt angle depends quasi-linearly on the pump power. Second, it starts from 0 for sample 2, whereas it starts from around 750mW for sample 1 which has stronger anchoring conditions. For this sample, it seems as if a threshold process would occur but this should be due to the low accuracy of the measurements (1 or 2 degrees) for small tilt angles: the actual tilt angle is possibly very small but not zero for low pump powers. Whatever this behavior is a true or a quasi threshold, it should be of great interest to obtain informations on anchoring conditions.

Also, on the two curves one can see an anomaly for pump powers around 1200mW, which is the region where we have already observed a clear change in the temperature profiles. The two phenomena are certainly correlated to each other but nothing is really clear at the moment and the question is still open.

CONCLUSION.

Quantitative investigations on Optical Frederiks Transition have been performed on homeotropically aligned nematic films with weak anchoring conditions and illuminated with a continuous wave under normal incidence, using Total Internal Reflection technique. The temperature profile within the pump beam has been measured and found much more wider than that of the pump beam. Modelling of these observations is under way. Also the director surface tilt angle in the center of the pump beam has been measured. For low pump powers, the obtained values depend linearly on the pump power. For one sample a thresholdlike behavior has been observed but that should be confirmed by further experiment. The obtained results on temperature should help to solve the very tricky differential equations that govern heat transfer and director distribution both on the surface and in the bulk. The observed director surface tilt angle behavior should lead to a new method for determining the anchoring conditions of a nematic film.

REFERENCES

1. See for example:
R. M. Herman and R. J. Serinko, Phys. Rev. A., 19,1757,(1979).
R. M. Herman and R. J. Serinko, Phys. Rev. A., 19,1757,(1979)
A. S. Zolot'ko, V. F. Kitaeva, N. Kroo, N.N. Sobolev and L. Chillag, JETP. Lett., 32, 158, (1980).
A. S. Zolot'ko, V. F. Kitaeva, N. N. Sobolev and L. Chillag, JETP. Lett., 32 (2), 158, (1980).
I. C. Khoo and S. L. Zhuang, Appl. Phys. Lett., 37, 3, (1980).
N. V. Tabiryan and B. Ya Zel'dovich, Mol. Cryst. Liq. Cryst., 62, 237, (1981); Mol. Cryst. Liq. Cryst., 69, 19, (1981); Mol. Cryst. Liq. Cryst., 69, 31, (1981).
I. C. Khoo, S. L. Zhuang and S. Shepard, Appl. Phys. Lett., 39(12), 937, (1981).
N. V. Tabiryan, A. V. Sukhov and B. Y. Zel'dovich, Mol. Cryst. Liq. Cryst., 136, 1, (1986).
I. C. Khoo, Prog. in Optics, XXVI, 105, (1988).
2. M. Warenghem and G. Joly, Mol. Cryst. Liq. Cryst., 207, 205, (1991).

3. D. Rivière, Y. Levy and C. Imbert, Opt. Comm., 25 (2), 206, (1978).
Y. Levy, D. Rivière, C. Imbert and M. Boix, Opt. Comm., 26 (2), 225, (1978).
4. M. Warenghem, M. Ismaili, D. Hector, J. de Phys. III, 2, 765, (1992).
5. K. Eidner, G. Mayer and R. Schuster, Phys. Lett. A, 118(3),149-151, (1986).
K. Eidner, G. Mayer and R. Schuster, Phys. Lett. A, 118(3),152-154, (1986).
6. F. Bloisi, L. Vicari and F. Simoni, Mol. Cryst. Liq. Cryst., 179, 45, (1990).
7. F. Simoni, F. Bloisi, L. Vicari, M. Warenghem, M. Ismaili and D. Hector, Europhys. Lett., 21(2), 189, (1993).
8. M. Warenghem, M. Ismaili, F. Simoni, F. Bloisi, L. Vicari, This issue.
9. R. Vilanove, E. Guyon, C. Mitescu and P. Pieranski, J. de Phys., 35, 153, (1974).
10. N. Tabiryan, private discussion.